

2017

Fluorogenic protein labeling using a genetically encoded unstrained alkene

Xin Shang

University of Nebraska-Lincoln, xshang3@unl.edu

X. Song

University of Nebraska - Lincoln

C. Faller

University of Nebraska - Lincoln

R. Lai

University of Nebraska - Lincoln

H. Li

University of Nebraska - Lincoln

See next page for additional authors

Follow this and additional works at: <https://digitalcommons.unl.edu/chemfacpub>

 Part of the [Analytical Chemistry Commons](#), [Medicinal-Pharmaceutical Chemistry Commons](#), and the [Other Chemistry Commons](#)

Shang, Xin; Song, X.; Faller, C.; Lai, R.; Li, H.; Cerny, R.; Niu, Wei; and Guo, Jiantao, "Fluorogenic protein labeling using a genetically encoded unstrained alkene" (2017). *Faculty Publications -- Chemistry Department*. 106.

<https://digitalcommons.unl.edu/chemfacpub/106>

This Article is brought to you for free and open access by the Published Research - Department of Chemistry at DigitalCommons@University of Nebraska - Lincoln. It has been accepted for inclusion in Faculty Publications -- Chemistry Department by an authorized administrator of DigitalCommons@University of Nebraska - Lincoln.

Authors

Xin Shang, X. Song, C. Faller, R. Lai, H. Li, R. Cerny, Wei Niu, and Jiantao Guo

Cite this: *Chem. Sci.*, 2017, 8, 1141

Fluorogenic protein labeling using a genetically encoded unstrained alkene†

X. Shang,^a X. Song,^a C. Faller,^a R. Lai,^a H. Li,^a R. Cerny,^a W. Niu^{*b} and J. Guo^{*a}

We developed a new fluorogenic bioorthogonal reaction that is based on the inverse electron-demand Diels–Alder reaction between styrene (an unstrained alkene) and a simple tetrazine. The reaction forms a new fluorophore with no literature precedent. We have identified an aminoacyl-tRNA synthetase/tRNA pair for the efficient and site-specific incorporation of a styrene-containing amino acid into proteins in response to amber nonsense codon. Fluorogenic labeling of purified proteins and intact proteins in live cells were demonstrated. The fluorogenicity of the styrene–tetrazine reaction can be potentially applied to the study of protein folding and function under physiological conditions with low background fluorescence interference.

Received 14th August 2016
Accepted 23rd September 2016

DOI: 10.1039/c6sc03635j

www.rsc.org/chemicalscience

Introduction

Selective labeling of proteins through fluorogenic bioorthogonal reactions is a powerful tool for studying protein structure and function.^{1–4} Fluorogenicity, which leads to good signal-to-noise ratio, is highly desirable for protein labeling in a complex biological environment. Fluorogenic bioorthogonal reactions, where the removal of unreacted reagents is not necessary, could simplify and, in some situations, enable real-time imaging experiments in live cells. One widely used strategy to design fluorogenic bioorthogonal reactions is based on the removal of a specific functional group that suppresses fluorescence of a fluorophore. In this case, the fluorescence quencher is also the reactive group on the reagent, *e.g.*, azide,^{5–8} alkyne,⁹ or tetrazine.^{10,11} This strategy has been applied to fluorogenic protein labeling.^{6,8,11} Another strategy is based on the simultaneous generation of a fluorophore through a bioorthogonal chemical transformation. Due to the challenging aspects in reaction design, this strategy is much less explored. One rare and elegant example is the light-induced 1,3-dipolar cycloaddition reaction between tetrazoles and terminal alkenes, which forms a fluorescent pyrazoline cycloadduct.^{12–14}

Here we report a fluorogenic bioorthogonal reaction between styrene and tetrazine. A new fluorophore with no literature precedent is formed in this reaction. In comparison to the fluorescence quencher-removal strategy, which turns a weak fluorescence signal into a stronger one, the fluorophore formation strategy likely gives lower background signal since

the bioconjugation product is the only fluorescent species within the entire system. While the styrene–tetrazine reaction is slower than reactions between strained alkenes and tetrazine,^{10,11,15–27} the good cellular stability and the fluorogenic property of the unstrained styrene make it an intriguing alternative to strained alkenes in bioconjugation applications with tetrazines.

Results and discussion

The fluorogenic styrene–tetrazine reaction

The fluorogenic property of the styrene–tetrazine reaction was discovered during our investigation of inverse electron-demand Diels–Alder (IEDDA) reactions between alkenes and tetrazines. The cycloaddition product of styrene and 3,6-dipyridin-2-yl-1,2,4,5-tetrazine (abbreviated as tetrazine hereafter), 4-phenyl-3,6-di(pyridin-2-yl)-1,4-dihydropyridazine (PDHP), represents a new fluorophore with no literature precedent (Fig. 1). The structure of the molecule was confirmed by both 1D and 2D ¹H NMR (Fig. S13 and S14†). Our study also showed that PDHP is a solvatochromic fluorophore (Fig. 1B). The absorption spectra and extinction coefficients (3769–4674 M^{−1} cm^{−1}) of PDHP are shown in Fig. S2.† The quantum yield of PDHP ranged from 0.011 to 0.251 in solvents of different polarity, which makes PDHP a potential candidate for the study of protein folding and conformational change. Comparing to some commonly used fluorophores²⁸ (Table S3†), PDHP has relatively low quantum yield and extinction coefficient. On the other hand, PDHP has a large Stokes shift, which could be beneficial (*e.g.*, less self-quenching and/or auto-fluorescence background) in certain imaging applications.

¹H NMR studies showed that PDHP was stable when stored in DMSO/D₂O (4 : 1) at room temperature for over 24 hours (Fig. S15†). When PDHP was incubated at 37 °C in PBS buffer (pH 7.4, 10% DMSO as cosolvent) in the presence of air, only

^aDepartment of Chemistry, University of Nebraska-Lincoln, Lincoln, NE 68588, USA. E-mail: jguo4@unl.edu

^bDepartment of Chemical & Biomolecular Engineering, University of Nebraska-Lincoln, Lincoln, NE 68588, USA. E-mail: wniu2@unl.edu

† Electronic supplementary information (ESI) available. See DOI: 10.1039/c6sc03635j



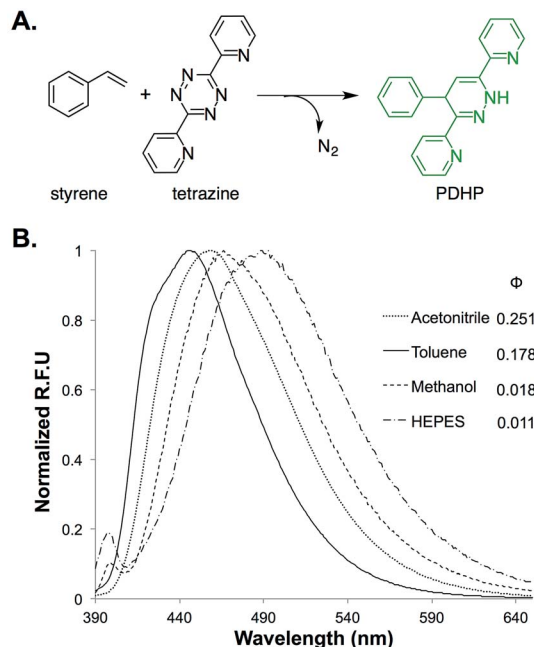


Fig. 1 (A) Fluorogenic reaction between styrene and tetrazine; (B) fluorescence properties of the bio-conjugation product, 4-phenyl-3,6-di(pyridin-2-yl)-1,4-dihydropyridazine (PDHP). $\lambda_{\text{ex}} = 360 \text{ nm}$.

a slow decay of fluorescence was observed (Fig. S3[†]). Data of the stability studies (Fig. S3[†]) also supports that PDHP, not the oxidation product of PDHP (4-phenyl-3,6-di(pyridin-2-yl)pyridazine), is the true fluorophore. To further characterize PDHP, we conducted pH-sensitivity studies. The emission spectra of PDHP were monitored in solutions of varied pH (Fig. S4B[†]). The fluorescence intensity peaked between pH 7 and pH 10, and decreased significantly when the pH was lower than 5. Notable changes in the absorbance spectrum of PDHP solution were also observed at the lower pH (Fig. S4A[†]). The fluorescence of PDHP was not affected by common nucleophiles in the biological system, such as cysteine and glutathione (Fig. S5[†]). This property makes the PDHP-forming styrene-tetrazine reaction compatible with protein labeling in live cells.

The fluorogenic mechanism of the styrene-tetrazine reaction is completely different from previously reported fluorogenic reactions involving tetrazine,¹¹ where the fluorescence quenching effect of tetrazine to a covalently linked fluorescent probe was exploited.²⁹ The loss of the tetrazine moiety results in the increase of the fluorescence signal from the probe. In comparison to this quencher-removal strategy, which turns a weak fluorescence signal into a stronger one, the *in situ* fluorophore-forming reaction between styrene and tetrazine has the minimal background signal since the conjugation product is the only fluorescent species within the entire system.

Reaction rate of the styrene-tetrazine reaction

To estimate if styrene-tetrazine reaction can be applied to the labeling of biomolecules in live cells, we conducted kinetics studies of the styrene-tetrazine reaction in methanol/water

(v/v 1 : 3). The pseudo-first-order rate constant (k_{obs}) was measured by monitoring the consumption of tetrazine in the presence of different concentrations of excess styrene. The second-order rate constant was determined by plotting k_{obs} against styrene concentrations. The styrene-tetrazine reaction ($k = 0.078 \text{ M}^{-1} \text{ s}^{-1}$) is faster than reactions between isolated terminal alkenes and tetrazines (entry 1–3, Table S1[†]).^{30–33} This observation is consistent with results of our quantum mechanical calculations (Table S2[†]), which showed that a C-substituent with π conjugation (*i.e.*, phenyl-) raised the HOMO energy of a terminal alkene.³⁴ HOMO (alkene) of higher energy level benefits an iEDDA reaction between an alkene and a tetrazine.^{35,36} Although the styrene-tetrazine reaction is slower than certain reactions between strained alkenes and tetrazine (entry 7, 8, 10, Table S1[†]),^{10,11,15–27} its rate is comparable to the strain-promoted cycloaddition of fluorinated cyclooctynes with azides³⁷ (entry 11, Table S1[†]) and the first generation of cyclopropene-tetrazine reaction (entry 9, Table S1[†]),²⁶ which have been successfully applied to the labeling of biomolecules in live cells.^{26,30,31,33,37}

Genetic incorporation of KStyr

In order to apply the fluorogenic bioorthogonal styrene-tetrazine reaction to protein labeling, a lysine-derived unnatural amino acid containing styrene moiety (KStyr; Fig. 2A) was synthesized. We screened a library of reported pyrrolysyl-tRNA synthetase (PylRS) mutants to identify ones that could aminoacylate an amber suppressor tRNA (tRNA_{CUA}) with KStyr in *E. coli*. The amber suppression efficiency was directly linked to the expression level of a GFP mutant (sfGFP-Asn149TAG) that has an amber nonsense codon at position Asn149.^{38,39} Among all the PylRS variants examined (Fig. S7[†]), three (BhcKRS,⁴⁰ DizPKRS-Y349F,⁴¹ and TCOKRS¹¹) supported the efficient synthesis of full-length sfGFP (Fig. 2B). The DizPKRS-Y349F mutant (L274A, C313S, Y349F)⁴¹ was chosen for future work. This synthetase displayed the best fidelity towards KStyr and good suppression efficiency. In the absence of KStyr, no sfGFP fluorescence was detected (Fig. 2B). In a large-scale (100 mL cell culture) expression experiment of the sfGFP mutant (sfGFP-N149KStyr) in

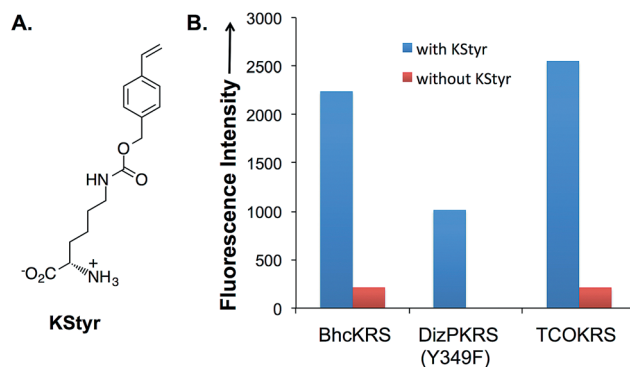


Fig. 2 Genetic incorporation of KStyr in *E. coli*. (A) Structure of KStyr (4-vinylbenzyl-*N*-carbamoyl-L-lysine); (B) fluorescence readings of cells expressing PylRS variants and a sfGFP-Asn149TAG mutant. The expressions were conducted either in the presence or in the absence of 0.5 mM KStyr. Fluorescence intensity was normalized to cell growth.



E. coli, 23 mg L⁻¹ of the fluorescent protein was obtained after partial purification using affinity chromatography (Fig. S8†). Mass spectrometry analyses of the purified protein (Fig. S9†) confirmed that KStyr was site specifically incorporated at position 149 of sfGFP.

In vitro protein labeling

We first conducted a series of labeling experiments to gauge the reaction between protein-borne styrene group and tetrazine reagent. A previously reported tetrazine–fluorescein reagent³⁰ (FL–Tet, Fig. S1†) was synthesized and used in these studies. Following labeling reactions of sfGFP-N149KStyr by FL–Tet, samples were boiled to denature the protein so that the only fluorescent species is the fluorescein conjugates. Protein band with fluorescence was detected 2 min after the reaction was initiated and the fluorescence intensity increased in a time-dependent manner (Fig. S10B†). Control experiments using wild-type sfGFP and FL–Tet, or sfGFP-N149KStyr only did not afford detectable labeling (Fig. S10†). These results demonstrate that the unnatural styrene moiety of KStyr is biocompatible and orthogonal to functional groups in natural amino acids.

Encouraged by the initial results, we further examined if the PDHP fluorophore generated from the styrene–tetrazine reaction could be directly detected in protein labeling experiments. We first examined the labeling of the sfGFP-N149KStyr mutant with varied concentrations of tetrazine in PBS buffer following a 10 min reaction (Fig. 3A). Weak fluorescence was detected when 100 μM of tetrazine was used. Significantly greater

fluorescence intensities were observed as tetrazine concentrations reached 250 μM or higher (Fig. 3A). A robust fluorogenic protein labeling was also observed in a time dependence study using 500 μM of tetrazine. As shown in Fig. 3B, fluorescence was detected 5 min after the reaction was initiated. The fluorescence intensity increased gradually in a time-dependent manner (Fig. 3B and S16†). No fluorescence was observed in control experiments when either wild-type sfGFP was used in the reaction or tetrazine was omitted in reactions involving sfGFP-N149KStyr. Based on mass spectrometry studies, the correct mass of sfGFP-N149KStyr protein after the labelling reaction was observed (calculated mass: 27 673; observed mass: 27 673; these masses are corresponding to protein without N-terminal methionine). Above results confirmed that this fluorogenic styrene–tetrazine reaction could be used as an efficient tool to selectively label a purified protein.

In vivo protein labeling

We demonstrated that the fluorogenic styrene–tetrazine reaction could be used to label an intracellular stress response protein, HdeA, in live cells. Plasmid pHdeA was constructed to

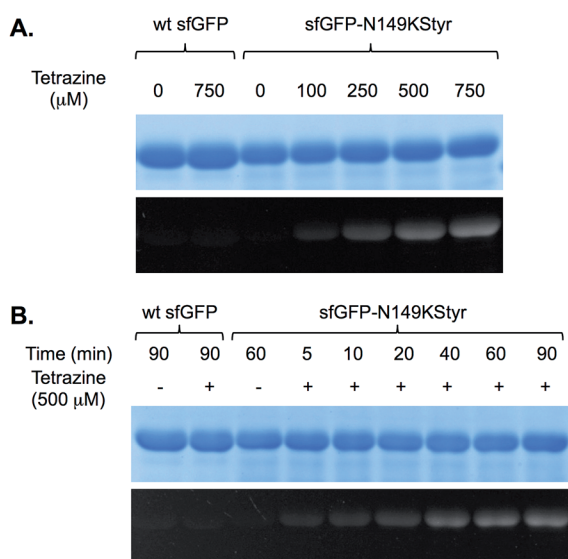


Fig. 3 Fluorogenic labeling of sfGFP variants with tetrazine. Following labeling reactions, protein samples were denatured by heating, then analyzed by SDS–PAGE. The top panel in each figure shows Coomassie blue stained gel and the bottom panel shows the fluorescent image of the same gel before Coomassie blue treatment. (A) Labeling of sfGFP-N149KStyr mutant with varied concentrations of tetrazine for 10 minutes. Protein samples (2.75 μg) after labeling reactions were analysed by SDS–PAGE; (B) reaction progress of sfGFP-N149KStyr labeling with 500 μM of tetrazine. Wild-type sfGFP was included in both experiments as the control.

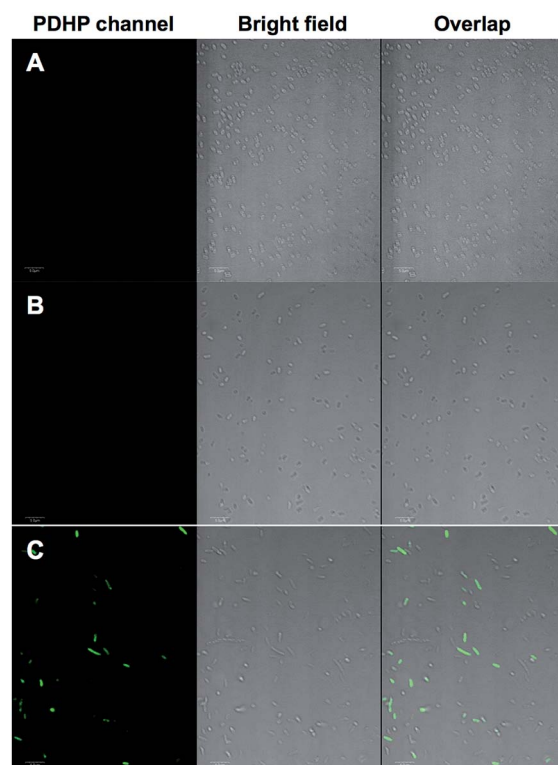


Fig. 4 Selective labeling of *E. coli* cells expressing HdeA-F28KStyr. (A) Wild-type HdeA that was expressed in the presence of KStyr; (B) HdeA-F28KStyr mutant that was expressed in the presence of KStyr but in the absence of DizPKRS-Y349F; (C) HdeA-F28KStyr mutant that was expressed in the presence of KStyr and DizPKRS-Y349F. For all images, the left panel shows fluorescent images of *E. coli* cells in PDHP channel (405 nm excitation and 505–540 nm emission), the middle panel shows bright-field images of the same *E. coli* cells, and the right panel shows composite images of bright-field and fluorescent images. Scale bars, 10 μm.



encode an HdeA mutant containing KStyr at position 28 (HdeA-F28KStyr). *E. coli* cells expressing HdeA-F28KStyr was washed and incubated with 100 μ M tetrazine for 1.5 hour at 37 °C. Cells were collected, directly re-suspended PBS buffer (without additional washing steps), and imaged. As shown in Fig. 4C, strong fluorescent signals that co-localized nicely with cells were detected. As a control, *E. coli* cells expressing wild-type HdeA in the presence of KStyr was washed and incubated with 100 μ M tetrazine under the same conditions. No fluorescence was observed (Fig. 4A). As a second control, fluorescence was also not detected from cells expressing HdeA-F28KStyr in the presence of KStyr but in the absence of DizPKRS-Y349F (Fig. 4B). The above two control experiments confirmed that the observed fluorescence signals in Fig. 4C were from labeled HdeA-F28KStyr mutant protein and not from free KStyr. In comparison to labeling reagents that are constantly fluorescent, the fluorogenic styrene-tetrazine reaction does not require an extra washing step to remove excess fluorescent reagents. Furthermore, the preparation of a bioorthogonal reagent-fluorophore conjugate is not needed, which simplifies the labeling of intracellular proteins.

Conclusions

In conclusion, a novel PDHP fluorophore with intriguing photophysical properties was formed from the styrene-tetrazine reaction. The successful genetic incorporation of a styrene-derived unnatural amino acid (KStyr) enabled site-specific and fluorogenic labeling of proteins both *in vitro* and *in vivo*. While the new PDHP fluorophore and its further application as an solvatochromic dye is still under investigation, the unique fluorogenic property of the styrene-tetrazine reaction could enable protein labeling in live cells without the need of extensive washing steps, which will likely have wide applications in biological studies. Given its ease of preparation, good cellular stability, and unique fluorogenic bioconjugation reaction with tetrazine, styrene serves as an intriguing alternative to strained alkenes for general labeling of biomolecules.

Acknowledgements

This work was supported by the New Faculty Startup Fund (to J. G.) from the University of Nebraska-Lincoln and the National Institute of Health (grant 1R01AI111862 to J. G.). The authors thank Dr Sophie Alvarez and Dr Mike Naldrett in the Proteomics & Metabolomics Facility at the Center for Biotechnology in University of Nebraska-Lincoln for help in protein mass spectrometry. The authors thank Dr You Zhou and Terri Fangman in the Microscopy facility at the Center for Biotechnology in University of Nebraska-Lincoln for help in fluorescence microscope analysis.

Notes and references

- 1 P. Shieh and C. R. Bertozzi, *Org. Biomol. Chem.*, 2014, **12**, 9307–9320.
- 2 K. Lang and J. W. Chin, *ACS Chem. Biol.*, 2014, **9**, 16–20.

- 3 C. P. Ramil and Q. Lin, *Chem. Commun.*, 2013, **49**, 11007–11022.
- 4 M. P. Bruchez, *Curr. Opin. Chem. Biol.*, 2015, **27**, 18–23.
- 5 K. Sivakumar, F. Xie, B. M. Cash, S. Long, H. N. Barnhill and Q. Wang, *Org. Lett.*, 2004, **6**, 4603–4606.
- 6 F. Friscourt, C. J. Fahrni and G.-J. Boons, *J. Am. Chem. Soc.*, 2012, **134**, 18809–18815.
- 7 P. Shieh, V. T. Dien, B. J. Beahm, J. M. Castellano, T. Wyss-Coray and C. R. Bertozzi, *J. Am. Chem. Soc.*, 2015, **137**, 7145–7151.
- 8 K. E. Beatty, J. C. Liu, F. Xie, D. C. Dieterich, E. M. Schuman, Q. Wang and D. A. Tirrell, *Angew. Chem., Int. Ed.*, 2006, **45**, 7364–7367.
- 9 Z. Zhou and C. J. Fahrni, *J. Am. Chem. Soc.*, 2004, **126**, 8862–8863.
- 10 N. K. Devaraj, S. Hilderbrand, R. Upadhyay, R. Mazitschek and R. Weissleder, *Angew. Chem., Int. Ed.*, 2010, **49**, 2869–2872.
- 11 K. Lang, L. Davis, S. Wallace, M. Mahesh, D. J. Cox, M. L. Blackman, J. M. Fox and J. W. Chin, *J. Am. Chem. Soc.*, 2012, **134**, 10317–10320.
- 12 Z. Yu, L. Y. Ho and Q. Lin, *J. Am. Chem. Soc.*, 2011, **133**, 11912–11915.
- 13 W. Song, Y. Wang, J. Qu, M. M. Madden and Q. Lin, *Angew. Chem., Int. Ed.*, 2008, **47**, 2832–2835.
- 14 Z. Yu, Y. Pan, Z. Wang, J. Wang and Q. Lin, *Angew. Chem., Int. Ed.*, 2012, **51**, 10600–10604.
- 15 A.-C. Knall and C. Slugovec, *Chem. Soc. Rev.*, 2013, **42**, 5131–5142.
- 16 M. L. Blackman, M. Royzen and J. M. Fox, *J. Am. Chem. Soc.*, 2008, **130**, 13518–13519.
- 17 N. K. Devaraj, R. Weissleder and S. A. Hilderbrand, *Bioconjugate Chem.*, 2008, **19**, 2297–2299.
- 18 M. Royzen, G. P. A. Yap and J. M. Fox, *J. Am. Chem. Soc.*, 2008, **130**, 3760–3761.
- 19 M. T. Taylor, M. L. Blackman, O. Dmitrenko and J. M. Fox, *J. Am. Chem. Soc.*, 2011, **133**, 9646–9649.
- 20 Y. Liang, J. L. Mackey, S. A. Lopez, F. Liu and K. N. Houk, *J. Am. Chem. Soc.*, 2012, **134**, 17904–17907.
- 21 D. S. Liu, A. Tangpeerachaiikul, R. Selvaraj, M. T. Taylor, J. M. Fox and A. Y. Ting, *J. Am. Chem. Soc.*, 2012, **134**, 792–795.
- 22 J. L. Seitchik, J. C. Peeler, M. T. Taylor, M. L. Blackman, T. W. Rhoads, R. B. Cooley, C. Refakis, J. M. Fox and R. A. Mehl, *J. Am. Chem. Soc.*, 2012, **134**, 2898–2901.
- 23 K. Lang, L. Davis, J. Torres-Kolbus, C. Chou, A. Deiters and J. W. Chin, *Nat. Chem.*, 2012, **4**, 298–304.
- 24 T. Plass, S. Milles, C. Koehler, J. Szymanski, R. Mueller, M. Wiessler, C. Schultz and E. A. Lemke, *Angew. Chem., Int. Ed.*, 2012, **51**, 4166–4170.
- 25 A. Borrmann, S. Milles, T. Plass, J. Dommerholt, J. M. M. Verkade, M. Wiessler, C. Schultz, J. C. M. van Hest, F. L. van Delft and E. A. Lemke, *ChemBioChem*, 2012, **13**, 2094–2099.
- 26 D. M. Patterson, L. A. Nazarova, B. Xie, D. N. Kamber and J. A. Prescher, *J. Am. Chem. Soc.*, 2012, **134**, 18638–18643.



- 27 J. Yang, J. Seckute, C. M. Cole and N. K. Devaraj, *Angew. Chem., Int. Ed.*, 2012, **51**, 7476–7479.
- 28 L. D. Lavis and R. T. Raines, *ACS Chem. Biol.*, 2008, **3**, 142–155.
- 29 N. K. Devaraj and R. Weissleder, *Acc. Chem. Res.*, 2011, **44**, 816–827.
- 30 Y.-J. Lee, Y. Kurra, Y. Yang, J. Torres-Kolbus, A. Deiters and W. R. Liu, *Chem. Commun.*, 2014, **50**, 13085–13088.
- 31 U. Rieder and N. W. Luedtke, *Angew. Chem., Int. Ed.*, 2014, **53**, 9168–9172.
- 32 J. W. Wijnen, S. Zavarise, J. B. F. N. Engberts and M. Charton, *J. Org. Chem.*, 1996, **61**, 2001–2005.
- 33 A. Niederwieser, A.-K. Spaete, L. D. Nguyen, C. Juengst, W. Reutter and V. Wittmann, *Angew. Chem., Int. Ed.*, 2013, **52**, 4265–4268.
- 34 I. Fleming, *Molecular Orbitals and Organic Chemical Reactions*, John Wiley & Sons Ltd, London, UK, 2009.
- 35 F. Liu, Y. Liang and K. N. Houk, *J. Am. Chem. Soc.*, 2014, **136**, 11483–11493.
- 36 F. Liu, R. S. Paton, S. Kim, Y. Liang and K. N. Houk, *J. Am. Chem. Soc.*, 2013, **135**, 15642–15649.
- 37 J. M. Baskin, J. A. Prescher, S. T. Laughlin, N. J. Agard, P. V. Chang, I. A. Miller, A. Lo, J. A. Codelli and C. R. Bertozzi, *Proc. Natl. Acad. Sci. U. S. A.*, 2007, **104**, 16793–16797.
- 38 P. R. Chen, D. Groff, J. Guo, W. Ou, S. Cellitti, B. H. Geierstanger and P. G. Schultz, *Angew. Chem., Int. Ed.*, 2009, **48**, 4052–4055.
- 39 N. Wang, T. Ju, W. Niu and J. Guo, *ACS Synth. Biol.*, 2015, **4**, 207–212.
- 40 J. Luo, R. Uprety, Y. Naro, C. Chou, D. P. Nguyen, J. W. Chin and A. Deiters, *J. Am. Chem. Soc.*, 2014, **136**, 15551–15558.
- 41 M. Zhang, S.-X. Lin, X.-W. Song, J. Liu, Y. Fu, X. Ge, X.-M. Fu, Z.-Y. Chang and P.-R. Chen, *Nat. Chem. Biol.*, 2011, **7**, 671–677.



Support Information

I. General material and method.....	2
II. Experimental procedure.....	3
III. Supplemental tables.....	9
IV. Supplemental figures	
1. Figure S1.....	11
2. Figure S2.....	12
3. Figure S3.....	13
4. Figure S4.....	14
5. Figure S5.....	15
6. Figure S6.....	16
7. Figure S7.....	17
8. Figure S8.....	18
9. Figure S9.....	19
10. Figure S10.....	20
11. Figure S11.....	21
12. Figure S12.....	22
13. Figure S13.....	23
14. Figure S14.....	24
15. Figure S15.....	25
16. Figure S16.....	26
IV. Reference.....	27

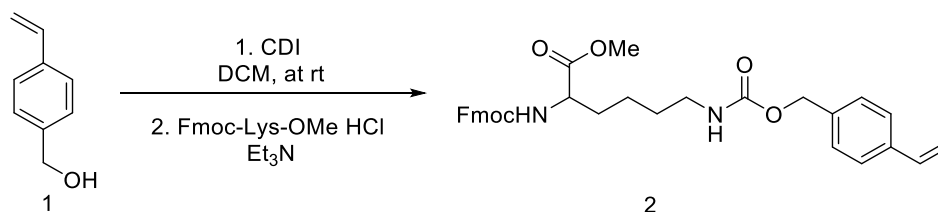
I. General material and method

Unless otherwise noted, starting materials, solvents and reagents for chemical synthesis were obtained from commercial suppliers (Acros, Alfa Aesar, Sigma-Aldrich, Chem-impex) and used without further purification. Dry solvents were either freshly distilled by following standard methods or directly purchased from Acros. Deuterated solvents were obtained from Sigma-Aldrich. Flash chromatography (FC) was carried out using SiliaFlash P60 (0.04–0.063 mm, 230–400 mesh) from Silicycle. Thin layer chromatography (TLC) was performed on glass-backed, precoated silica gel plates (Analtech). NMR spectra were recorded at 25 °C using a Bruker Advance III-HD 400 MHz NMR. Chemical shifts were reported in ppm with deuterated solvents as internal standards (CDCl_3 , H 7.26, C 77.0; DMSO-d_6 , H 2.50, C 39.5; D_2O , 4.79). Multiplicity was reported as follows: s = singlet, d = doublet, t = triplet, q = quartet, m = multiplet, b = broad. UV absorbance measurements for kinetic studies were conducted on Shimadzu UV2401-PC. Absorbance spectrum and intensity were measured on Shimadzu UV2401-PC and Thermo Scientific GENESYS 10S UV/Vis Spectrophotometer. Fluorescence spectrum and intensity were recorded on Horiba FluoroMax 4 spectrometer and BioTek Synergy H1 Hybrid plate reader. Sodium dodecyl sulfate-polyacrylamide gel electrophoresis (SDS-PAGE) was performed on Bio-Rad mini-PROTEAN electrophoresis system. Bio-Rad Prestained Protein Ladder was applied to at least one lane of each gel for the estimation of apparent molecular weights. Protein gels were stained by Coomassie Brilliant Blue staining and visualized using Bio-Rad Molecular Imager ChemiDoc XRS+ System. For in-gel fluorescence imaging, either Bio-Rad Molecular Imager ChemiDoc XRS+ System or GE Typhoon FLA9500 was used. Live cells were imaged on Olympus FV500 inverted (Olympus IX-81) confocal microscope.

II. Experimental procedures

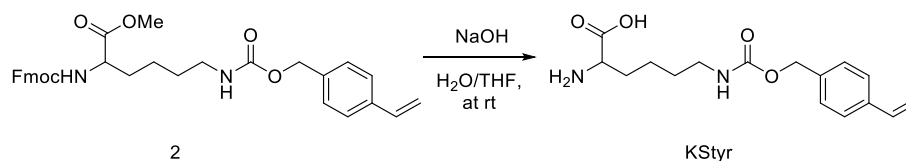
Synthetic procedures

N^α-(9-Fluorenylmethoxycarbonyl)-N^ε-(((4-vinylbenzyl)oxy)carbonyl)-L-lysine methyl ester (2):



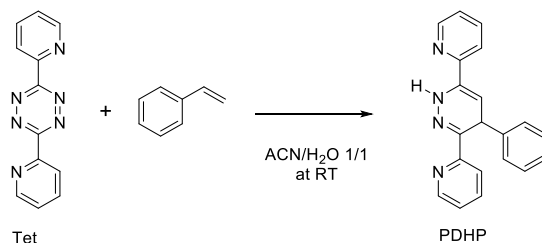
To the solution of 4-vinylbenzyl alcohol (**1**)¹ (268mg, 2.0 mmol) in 5 mL dry dichloromethane, 1,1'-carbonyldiimidazole (CDI; 356mg, 2.2 mmol) dissolved in 5 mL dichloromethane was added with stirring at 0 °C. After the formation of white precipitate, the suspension was kept stirring at room temperature for 1 hour. A solution of N^α-(fmoc)-L-lysine methyl ester hydrochloric acid salt (838 mg, 2 mmol) in a mixture of triethylamine (Et₃N, 279 μL, 2 mmol) and dichloromethane (DCM, 10 mL) was added to the stirred suspension dropwise. The resulting clear mixture was stirred at room temperature overnight. Following addition of 30 mL dichloromethane, the reaction mixture was washed with 1 N HCl, saturated NaHCO₃, and brine sequentially. Resulting solution was dried over Na₂SO₄ and concentrated under vacuum. The residue was further purified by silica gel flash chromatography (dichloromethane/methanol, from 100/1 to 50/1, v/v). Compound **2** (577 mg) was obtained as white solid in 53% yield. ¹H-NMR (400 MHz, CDCl₃) δ 7.76 (d, *J* = 7.5 Hz, 2H), 7.59 (d, *J* = 7.5 Hz, 2H), 7.28-7.50 (m, 8H), 6.69 (dd, *J* = 10.8, 17.6 Hz, 1H), 5.73 (d, *J* = 17.6 Hz, 1H), 5.36 (br, 1H), 5.25 (d, *J* = 10.8 Hz, 1H), 5.06 (s, 2H), 4.78 (s, 1H), 4.30-4.55 (m, 3H), 4.21 (t, *J* = 6.7 Hz, 1H), 3.75 (s, 3H), 3.19 (m, 2H), 1.30-1.80 (m, 6H). ¹³C-NMR (400 MHz, CDCl₃) δ 173.0, 156.6, 156.1, 144.0, 143.9, 141.4, 137.6, 136.5, 136.2, 128.5, 127.8, 127.2, 126.5, 126.3, 125.2, 120.1, 114.3, 67.1, 66.5, 53.7, 52.6, 47.3, 40.9, 32.3, 29.5, 22.4. HRMS (ESI) calcd for C₃₂H₃₄N₂O₆, [M + H]⁺ 543.2490, found 543.2489.

N^ε-(((4-vinylbenzyl)oxy)carbonyl)-L-lysine (KStyr):



N^{α} -Boc- N^{ϵ} -(4-vinylphenyl)carbamoyl-L-lysine methyl ester hydrochloric acid (**2**) (69 mg, 0.13 mmol) was dissolved in tetrahydrofuran (1.3 mL). Sodium hydroxide aqueous solution (0.64 mL, 1 N) was added dropwise with stirring. The mixture was stirred overnight at room temperature, then diluted with water and washed with diethyl ether for five times. The pH of the aqueous layer was adjusted to 7 to afford white precipitate. Vacuum filtration afforded 28 mg KStyr in 72% yield. $^1\text{H-NMR}$ (400MHz, 0.5N NaOH/D₂O) δ 7.53 (d, J = 8.0 Hz, 2H), 7.40 (d, J = 8.0 Hz, 2H), 6.81 (dd, J = 11.2, 17.6 Hz, 1H), 5.76 (d, J = 17.6 Hz, 1H), 5.35 (d, J = 11.2 Hz, 1H), 5.12 (s, 2H), 3.00-3.15 (m, 3H), 1.30- 1.70 (m, 6H). $^{13}\text{C-NMR}$ (100 MHz, D₂O/H₂O/0.2N NaOH) δ : 183.7, 168.4, 158.7, , 137.4, 136.3, 128.1 , 126.5 , 114.7, 66.5, 56.0, 40.4, 34.4, 28.9, 22.3. HRMS (ESI) calcd for C₁₆H₂₂N₂O₄, [M + H]⁺ 307.1653, found 307.1647.

4-phenyl-3,6-di(pyridin-2-yl)-1,4-dihydropyridazine (PDHP)



The solution of 3,6-di-2-pyridinyl-1,2,4,5-tetrazine² (Tet, 94mg, 0.4 mmol) in 100 mL of acetonitrile (CH₃CN) in water (50:50) was bubbled with Argon under stirring for 30 minutes. Five equivalents of styrene (229 μL , 2 mmol) were added into the solution. The resulting pink mixture was stirred overnight to form yellow solid, which was collected by vacuum filtration as desired product. To improve the final yield, the filtrate was extracted by diethyl ether (3 \times 50 mL). Combined organic layers were dried over Na₂SO₄. The solvent was removed by vacuum evaporation. The residue was further purified by flash chromatography with ethyl acetate/hexane (10% to 25%) to afford a yellow solid. PDHP (111 mg) was obtained in 89% yield by combining two portions of yellow solid. $^1\text{H-NMR}$ (400 MHz, CDCl₃) δ 9.34 (s, 1H), 8.55 (dd, J = 4.7, 14.3 Hz, 2H), 8.09 (d, J = 8.0 Hz, 1H), 7.67-7.69 (m, 2H), 7.62 (t, J = 9.1 Hz, 1H), 7.41 (d, J = 7.9 Hz, 2H), 7.21-7.27 (m, 3H), 7.14 (t, J = 6.3 Hz, 2H), 5.80-5.83 (m, 1H), 5.56 (d, J = 6.2 Hz, 1H). $^{13}\text{C-NMR}$ (100 MHz, CDCl₃) δ 155.1, 150.4, 148.4, 148.3, 144.0, 142.0, 136.5, 136.1, 135.9, 128.5, 128.0, 126.5, 123.0, 122.6, 121.0, 118.9, 99.0, 36.8. HRMS (ESI) calcd for C₂₀H₁₇N₄, [M + H]⁺ 313.1448, found 313.1442

Quantum yield determination

Quantum yields (ϕ) of PDHP in different solvents were determined by following a reported procedure.³ Quinine sulfate in 0.1 M H₂SO₄ was used as the standard to calculate ϕ value.⁴

Kinetic measurements.

The reactions were carried out in indicated solvent under pseudo first-order conditions with 10- to 50-fold excess of styrene and 0.1 mM tetrazine. Tetrazine stock solution (0.2 mM) in 20% methanol aqueous solution and 10 mM styrene stock in 30% methanol aqueous solution were prepared and the two stock solutions were mixed freshly into quartz cuvettes before UV measurement. The consumption of tetrazine was recorded by measuring tetrazine absorbance (A) at 530 nm at 21°C in 30 minutes. The pseudo first-order rate constant k_{obs} (s⁻¹) is the slope of a linear plot of the natural log of absorbance, ln(absorbance), against time (t). Triplet independent measurements were carried out for k_{obs} measurements. The second-order rate constant k_2 (M⁻¹s⁻¹) is the slope of calibration curves generated by plotting k_{obs} (s⁻¹) against styrene concentration (M⁻¹).

Computational methodology

All the quantum mechanical (QM)/FixSol⁵ calculations were performed by using the Quantum chemistry Polarizable force field program (QuanPol)⁶ implemented in the General Atomic and Molecular Electronic Structure System (GAMESS).⁷ The geometry optimizations were performed by using QM/FixSol¹ methods with density functional theory (DFT). In the calculations, B3LYP (Becke, three-parameter, Lee-Yang-Parr) exchange-correlation functional⁸ and the 6-31++G(d,p)⁸ basis set were used. The solvent effect was described with the FixSol model with a dielectric constant of 78.39.

Plasmid construction.

pHdeA-F28TAG. HdeA gene was PCR amplified from *E. coli* genomic DNA. An amber mutation (F28TAG) was introduced by site-directed mutagenesis. The HdeA-F28TAG gene was digested with *Nde*I and *B*l

I

, and ligated into pLei-GFP⁹ vector, which was treated with the

same restriction enzymes, to afford pHdeA-F28TAG. Plasmid pHdeA-F28TAG was confirmed by DNA sequencing.

psfGFP-N149TAG. The sfGFP-N149TAG gene was assembled by overlapping PCR using pLei-sfGFP-Y66TAG plasmid¹⁰ as the template. The digested PCR product was inserted into pLei⁹ vector behind a T5 promoter to afford plasmid psfGFP-N149TAG. Following were primers used in the construction:

P1: 5'-GAGGAGAAATTACATATGTCCAAG-3'

P2: 5'- AGTGAGGGTAGTTACCAGGGT-3'

P3: 5'-ACCCTGGTAACTACCCTCACTtatGGTGTCCAGTGCTTCTCTCG-3'

P4: 5'-GAGTCCAAGCTCAGCGGTG-3'

P5: 5'-GTGGCTATTGAAGTTATACTCCA-3'

P6: 5'-TGGAGTATAACTTCAATAGCCACtagGTGTACATCACTGCTGATAAACAG-3'

psfGFP-wt. The plasmid was constructed by site-directed mutagenesis using psfGFP-N149TAG as the template. Following primers were used.

P7 5'-TGGAGTATAACTtcAATAGCCACaatGTGTACATCACTGCTGATAAACAG-3'

P8 5'-CTGTTTATCAGCAGTGATGTACACattGTGGCTATTGAAGTTATACTCCA-3'

Screening of pyrrolysyl-tRNA synthetase variants for the genetic incorporation of KStyr.

A plasmid encoding a pyrrolysyl-tRNA synthetase (PylRS) mutant of interest was co-transformed with pLei-sfGFP-N149TAG into *E. coli* GeneHog.⁹ The resulting strain was inoculated into 1 mL of LB media with kanamycin (Kan, 50 mg/L) and chloramphenicol (Cm, 34 mg/L). Cells were cultured at 37 °C with shaking overnight. The seed culture (80 µL) was used to inoculate four cultures in fresh LB media (0.8 mL) containing Kan (50 mg/L), Cm (34 mg/L), and IPTG (0.25 mM). Two cultures also contained KStyr (1 mM). Following cultivation at 37 °C with shaking for 24 hours, cells were collected by centrifugation, washed with PBS buffer. and resuspended in 0.8 mL PBS for fluorescence and OD₆₀₀ measurements using a Synergy H1 Hybrid plate reader. The fluorescence of sfGFP was monitored with $\lambda_{Ex} = 480$ nm and $\lambda_{Em} =$

510 nm. The cell density was estimated by measuring the sample absorbance at 600 nm. Fluorescence intensities were normalized to cell growth. A total of 19 pyrrolysyl-tRNA synthetase mutants were characterized.

Protein expression and purification.

E. coli GeneHog strain harboring plasmid pBK-mutant 10 and psfGFP-N149TAG was cultured in 100 mL LB media containing Kan (50 mg/L) and Cm (34 mg/L) at 37 °C with shaking. The protein expression was induced at OD₆₀₀ of 0.6 by the additions of IPTG (0.25 mM) and KStyr (0.5 mM). Following an additional 16 h of cultivation, cells were collected by centrifugation at 5,000g and 4 °C for 15 min. Harvested cells were resuspended in lysis buffer containing potassium phosphate (20 mM, pH 7.4), NaCl (150 mM), and imidazole (10 mM). Cells were subsequently disrupted by sonication. Cellular debris was removed by centrifugation (21,000g, 30 min, 4 °C). The cell-free lysate was applied to Ni Sepharose 6 Fast Flow resin (GE Healthcare). Protein purification followed manufacturer's instructions. Protein concentrations were determined by Bradford assay (Bio-Rad). Purified protein was desalted prior to MS analysis.

Protein mass spectrometry

For full-length protein, the samples were directly analyzed by mass spectrometer. For protein fragment, gel band containing sfGFP-N149KStyr was cut from SDS-PAGE gel stained by Coomassie blue. After in-gel digestion with trypsin, the protein sample was dried down and re-dissolved in 120 µL of aqueous solution with 2.5% acetonitrile and 0.1% formic acid. A 5 µL of the digest sample was injected into a nano-LC-MS/MS that was equipped with a 0.075 mm x 250 mm C18 Dionex column and a Q-Exactive HF mass spectrometer.

The mass spectrometry data was analyzed using Mascot (Matrix Science, London, UK; version 2.5.1). Mascot was set up to search KStyr-containing peptide, LEYNFNSH-KStyr-VYITADK. Deamidation of asparagine and glutamine, oxidation of methionine were specified in Mascot as variable modifications. The MS/MS spectra were searched by Mascot using a fragment ion mass tolerance of 0.060 Da and a parent ion tolerance of 10.0 PPM (Figure S9). The Mascot results were loaded into Scaffold (version Scaffold_4.4.8, Proteome Software Inc., Portland, OR) to validate the MS/MS-based peptide and protein identifications.¹¹

Labeling of purified proteins.

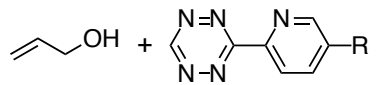
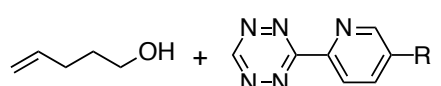
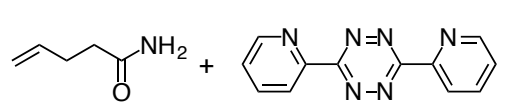
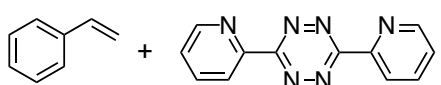
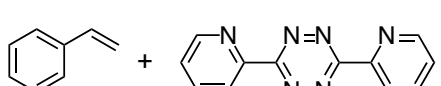
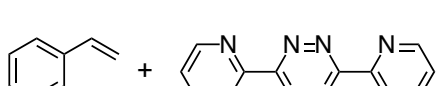
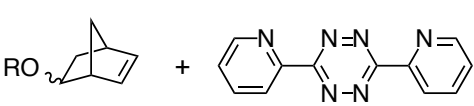
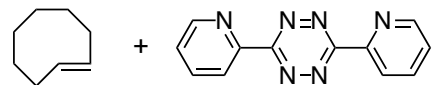
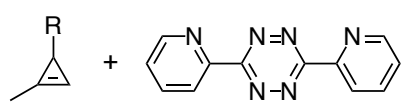
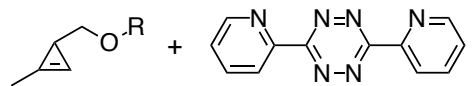
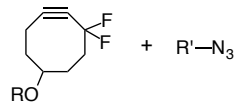
sfGFP-N149KStyr (9 μ L, 1 mg/mL) in PBS buffer was treated with 1 μ L of FL-Tet or Tet (in DMSO) at indicated concentrations. The reaction mixture was incubated at 37 $^{\circ}$ C with agitation for indicated period of time. Solution of 5-norbornene-2-methanol (10 μ L, 100 mM) in DMSO/PBS (1:9) was added to quench the reaction. The quenched reaction was then mixed with SDS-PAGE sample loading buffer (2x) and heated at 95 $^{\circ}$ C for 15 minutes. SDS-PAGE analysis followed manufacture's instruction. Fluorescence detection was performed before staining by Coomassie blue. Protein gels of Tet-labeled protein samples were imaged using Bio-Rad Molecular Imager ChemiDoc XRS+. Protein gels of FL-Tet-labeled protein samples were imaged using GE Typhoon FLA9500. Coomassie blue-stained gels were imaged using Bio-Rad Molecular Imager. As a control, wild-type sfGFP (9 μ L, 1 mg/mL) was subjected to labeling and analysis under the same conditions.

Labeling and imaging of live cells.

E. coli cells expressing either wild-type HdeA or HdeA-KStyr mutant proteins were harvested by centrifugation (21,000 g, 5 min, 4 $^{\circ}$ C). Collected cells were washed three times in the same volume of PBS by vortexing for 5 min. Washed cells were re-suspended in PBS buffer containing 5% glycerol. Tet stock solution was added into cell suspension to a final concentration of 100 μ M. After incubation for 90 min at 37 $^{\circ}$ C with agitation, cells were collected by centrifugation (21,000 g, 5 min, 4 $^{\circ}$ C) and resuspended in PBS buffer. Cell suspensions were placed on the surface of a glass slide and covered with a glass cover slip for imaging. Cells were imaged on an Olympus FV500 inverted (Olympus IX-81) confocal microscope. PDHP channel was excited by DAPI excitation wavelength (405 nm) and imaged using GFP emission filter (510 nm).

III. Supplemental tables

Table S1. Reaction rate comparison.

entry	reaction	Second-order rate constant k ($M^{-1} s^{-1}$)
1		0.0094 (in PBS buffer) ¹²
2		0.036 (in PBS buffer) ¹²
3		0.0042 (in 1:1 methanol/water) ¹³
4		0.048 (in 1:1 methanol/water) ¹³
5		0.078 (in 1:3 methanol/water; this work)
6		0.131 (in 95:5 water/t-BuOH) ¹⁴
7		1.0 (in 5:95 methanol/water) ¹⁵
8		2000 (in 9:1 methanol/water) ¹⁶
9		0.05 (in 1:1 CH ₃ CN/PBS) ¹⁷
10		2.8 (in 15:85 DMSO/PBS) ¹⁸
11		0.076 (in CH ₃ CN) ¹⁹

Note: These rate constants were measured in different solvents using different methods. The comparison is not absolute.

Table S2. Quantum mechanical calculations of HOMO energies of alkenes.

molecules	HOMO energy (Hartree)
5-hexenol	-0.2526
styrene	-0.2276

Table S3. The photophysical properties of some common fluorophores.²⁰

fluorophore	solvent	λ_{ex} (nm)	λ_{em} (nm)	Stokes shift (nm)	ϵ ($\text{M}^{-1}\text{cm}^{-1}$)	ϕ
PDHP	MeOH	360	465	105	4329	0.018
PDHP	CH ₃ CN	360	455	95	3769	0.251
7-Amino-4-methylcoumarin	MeOH	351	430	79	18000	0.75
NBD	MeOH	465	535	70	22000	0.3
fluorescein	pH 9	490	514	24	93000	0.95

IV. Supplemental figures

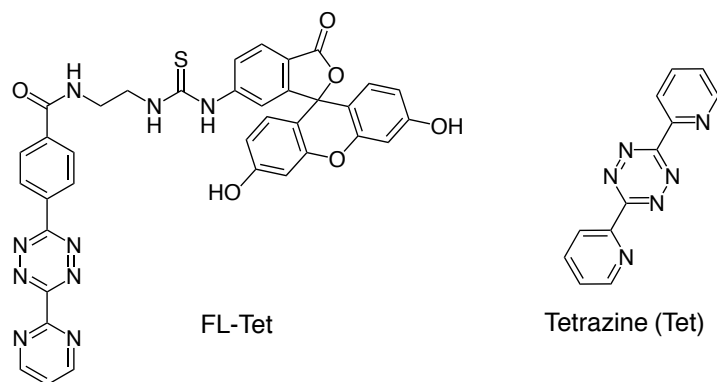


Figure S1. Structures of labeling reagents FL-Tet and tetrazine (Tet). Both compounds were synthesized by following reported procedures. Structures of synthesized compounds were confirmed by ¹H NMR.

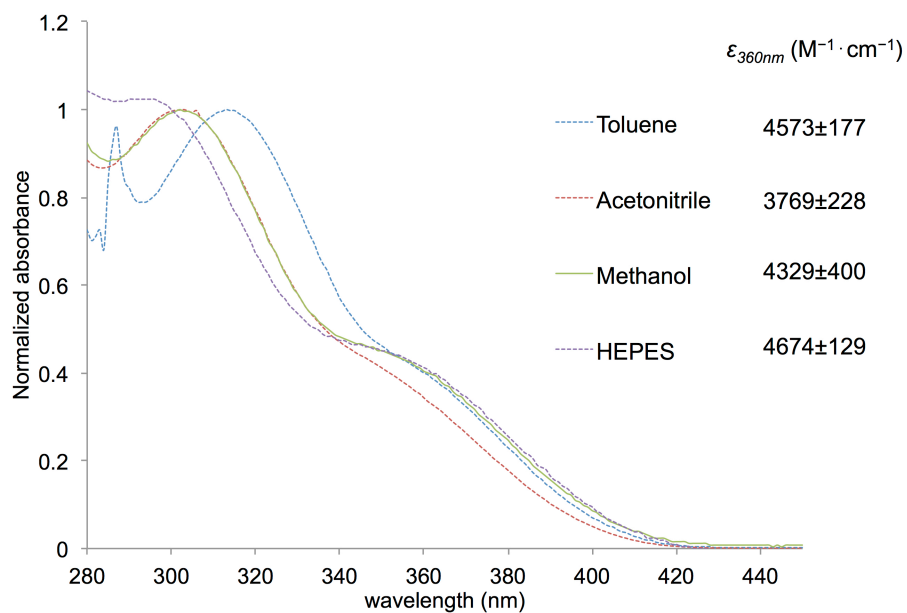


Figure S2. Absorbance spectra and extinction coefficients of PDHP in different solvents. HEPES: 4-(2-hydroxyethyl)-1-piperazineethanesulfonic acid; HEPES buffer contains 5% DMSO as cosolvent to improve the solubility of PDHP.

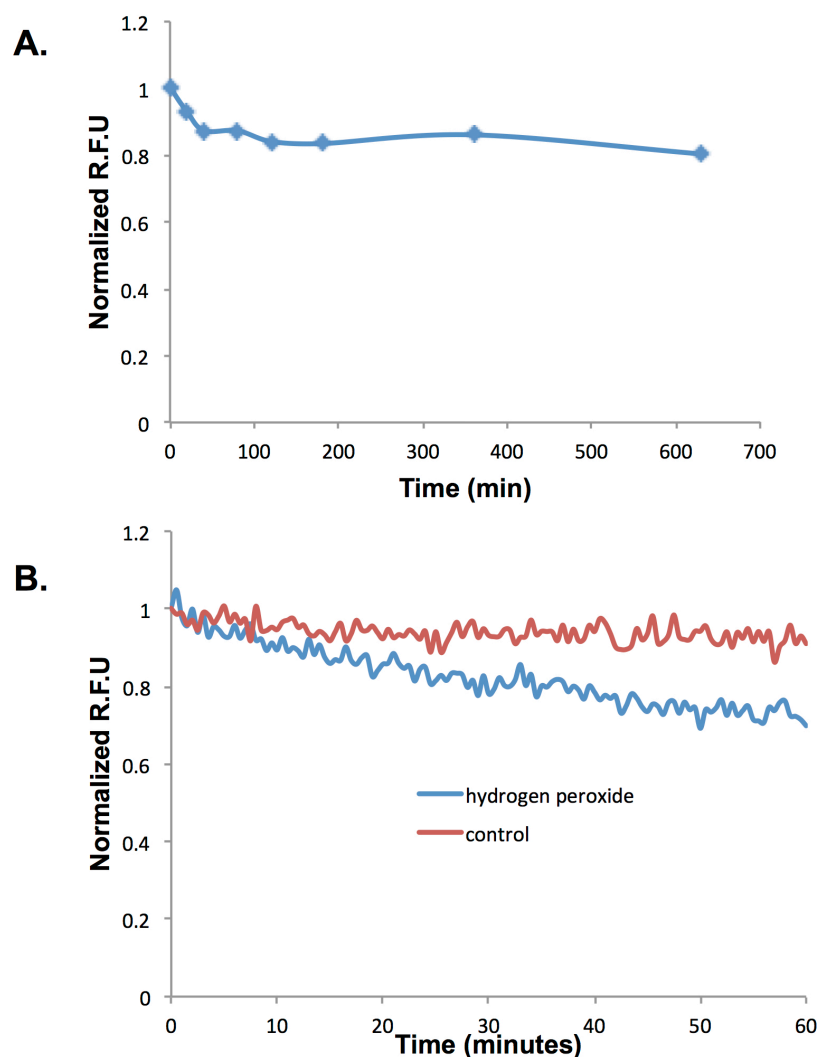


Figure S3. Fluorescence decay of PDHP in PBS buffer in the presence of air or H₂O₂. (A) Fluorescence decay of PDHP with shaking at 37 °C in the presence of atmospheric air. 5 mL of 10 μM PDHP solution in PBS buffer (with 10% DMSO) was incubated at 37 °C with shaking (250 rpm). At an indicated time point, a 100 μL solution was mixed with 100 μL of acetonitrile, and the fluorescence intensity was measured ($\lambda_{\text{Ex}} = 360 \text{ nm}$ and $\lambda_{\text{Em}} = 490 \text{ nm}$.) using a BioTek Synergy H1 Hybrid plate reader; (B) Fluorescence decay of PDHP stored in cuvette at room temperature (21 °C) in the presence of H₂O₂. After addition of H₂O₂ (2 μL, 200 mM), the PDHP solution (2 mL, 10 μM) in PBS buffer (with 10% DMSO) was excited at 360 nm and the intensity of emitted fluorescence light at 490 nm was recorded using a Horiba FluoroMax 4 spectrometer every 30 seconds.

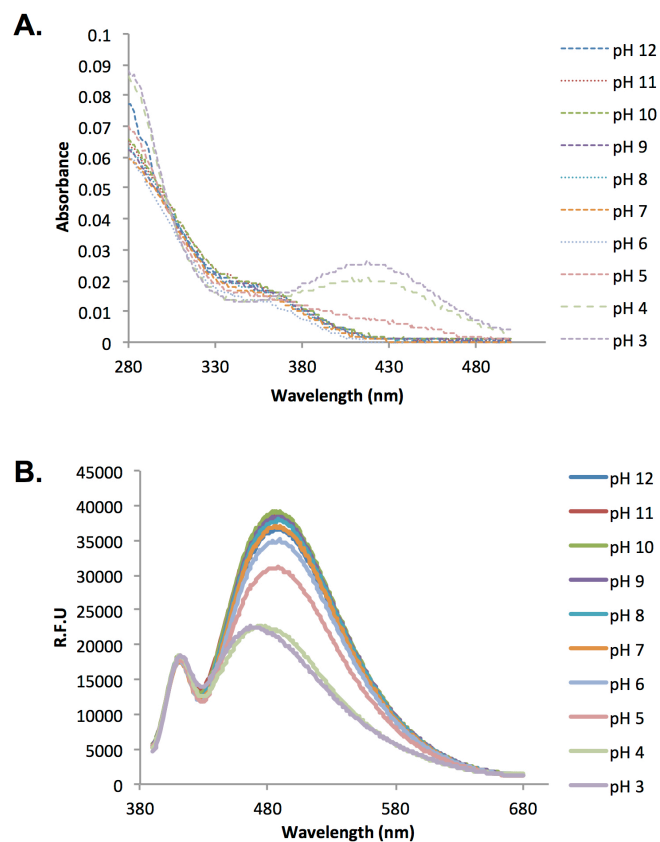


Figure S4. PDHP absorbance and emission spectrum at different pH. Buffers of different pH were prepared by mixing 0.04 M Britton-Robinson buffer (0.04 M acetic acid, 0.04 M phosphoric acid, and 0.04 M boric acid) with 0.2 M NaOH solution at appropriate ratios. All buffered aqueous solutions of PDHP (5 μ M) contain 10% DMSO as the cosolvent.

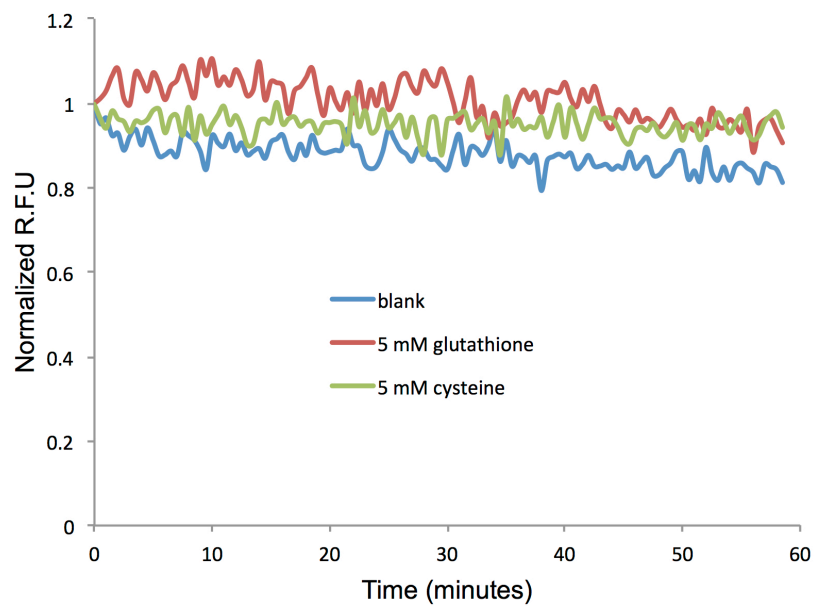


Figure S5. PDHP fluorescence in the presence of cysteine and glutathione. PDHP (20 μ M) was incubated with each reagent (5 mM) in PBS buffer (pH 7.4, 20% MeOH) at 21°C. Fluorescence was recorded every 30 seconds using a Horiba Fluoromax 4 spectrometer. Control experiment was carried out without the addition of reagents.

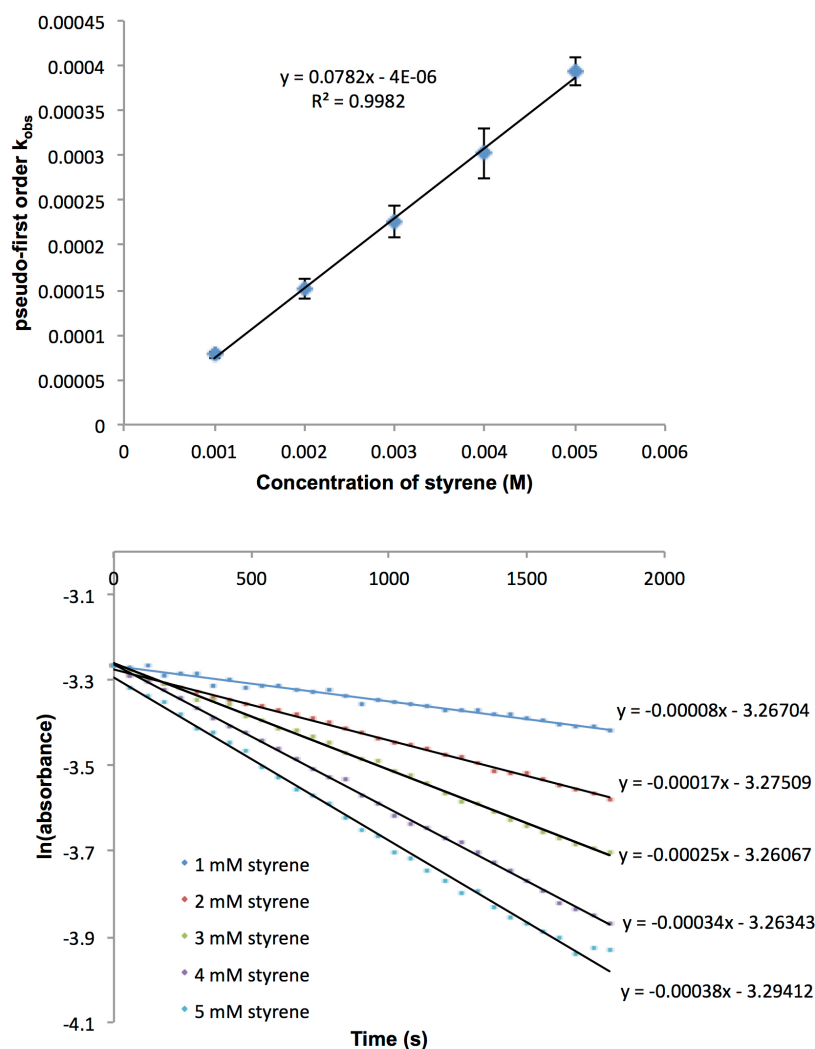


Figure S6. Kinetic studies of styrene-tetrazine reaction in MeOH/H₂O (1:3) solution. (A) Plots of $\ln(\text{absorbance})$ of tetrazine against time in reactions with varied concentrations of excess styrene. The slope of the linear curve is the pseudo-first-order rate constant k_{obs} (s⁻¹). The graph represents one dataset of three replicates; (B) Plot of the pseudo-first-order rate constant k_{obs} (s⁻¹) against the concentration of styrene. The slope of the linear curve is the second-order rate constant (M⁻¹s⁻¹) of this reaction. The error bar represents the standard deviation from triplicate measurements.

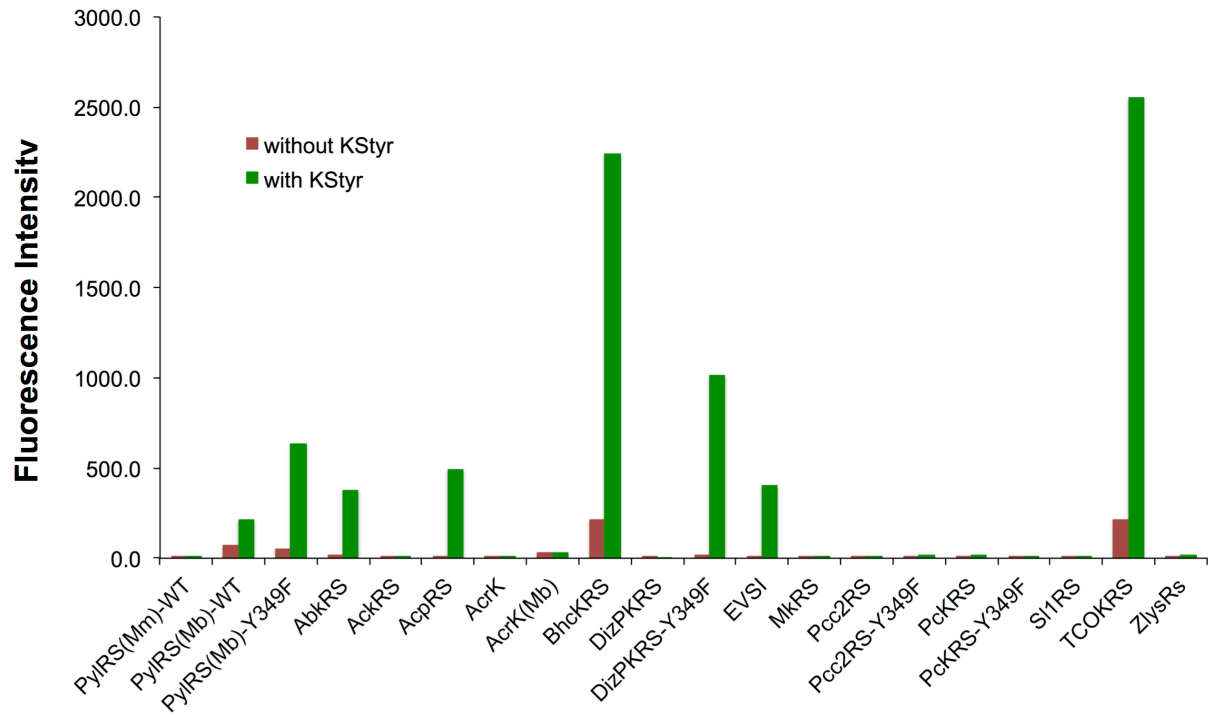


Figure S7. Screening of PyIRS mutants using GFP fluorescence assays. Fluorescence intensity was normalized to cell growth.

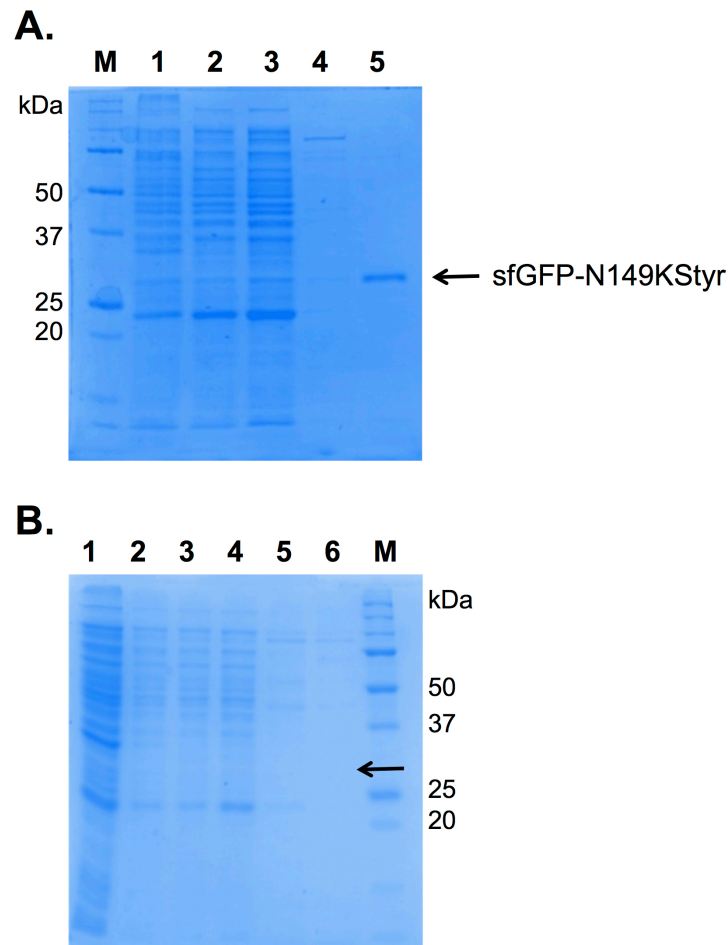


Figure S8. Protein purification and SDS-PAGE analysis. (A) Protein expression (in the presence of 0.5 mM KStyr), purification (through affinity chromatography using Ni-NTA resin), and SDS-PAGE analysis of sfGFP-N149TAG. Lane 1, total soluble proteins after sonication; 2 flow-through fraction; 3, first wash fraction; 4, second wash fraction; 5, elution. The purified sfGFP-N149KStyr is indicated with an arrow (27.6 kDa), and the protein yield is 23 mg/L; (B) Protein expression (in the absence of KStyr), purification (through affinity chromatography using Ni-NTA resin), and SDS-PAGE analysis of sfGFP-N149TAG. Lane 1, total soluble proteins after sonication; 2 flow-through fraction; 3, first wash fraction; 4, second wash fraction; 5, first elution; 6. Second elution. No full-length sfGFP mutant protein was observed.

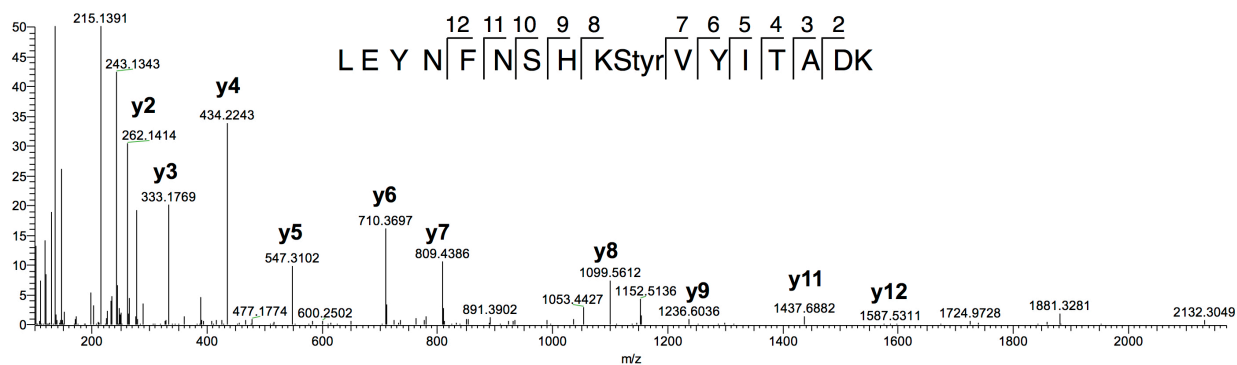


Figure S9. Mass spectrometry analysis of sfGFP-N149KStyr. The y ions are marked in the spectrum. The amino acid sequence of the peptide fragment, LEYNFNSH-KStyr-VYITADK, from mutant sfGFP containing KStyr is shown on top.

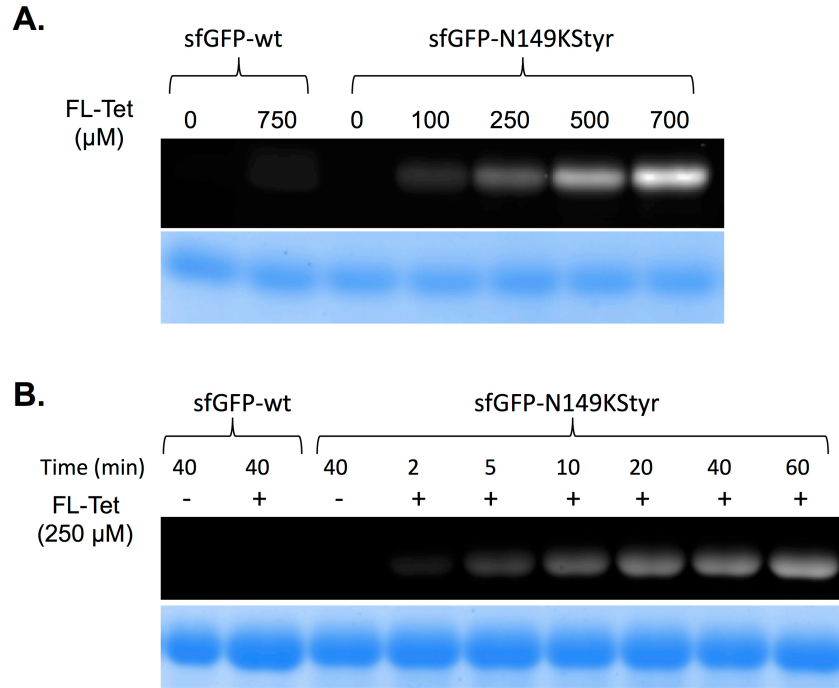


Figure S10. Labeling of sfGFP variants with FL-Tet. Wild-type sfGFP was included in both experiments as the control. Following labeling reactions, protein samples were denatured by heating, then analyzed by SDS-PAGE. The bottom panel in each figure shows Coomassie blue stained gel and the top panel shows the fluorescent image of the same gel (by GE Typhoon imager; Excitation/Emission filter: LPB (510LP)) before Coomassie blue treatment. (A) Labeling of sfGFP-N149KStyr with varied concentrations of FL-Tet for 5 minutes; (B) Reaction progress of sfGFP-N149KStyr labeling with 250 μ M of FL-Tet.

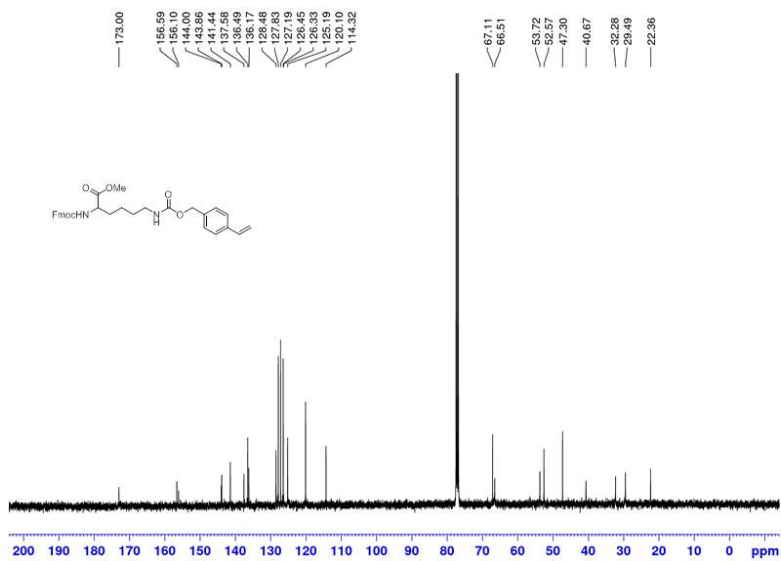
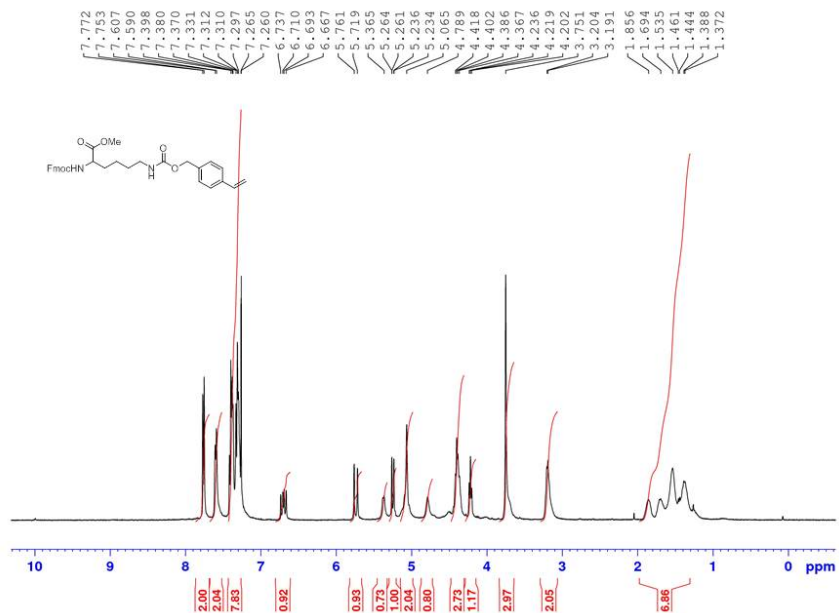


Figure S11. ¹H and ¹³C NMR spectra of protected KStyr.

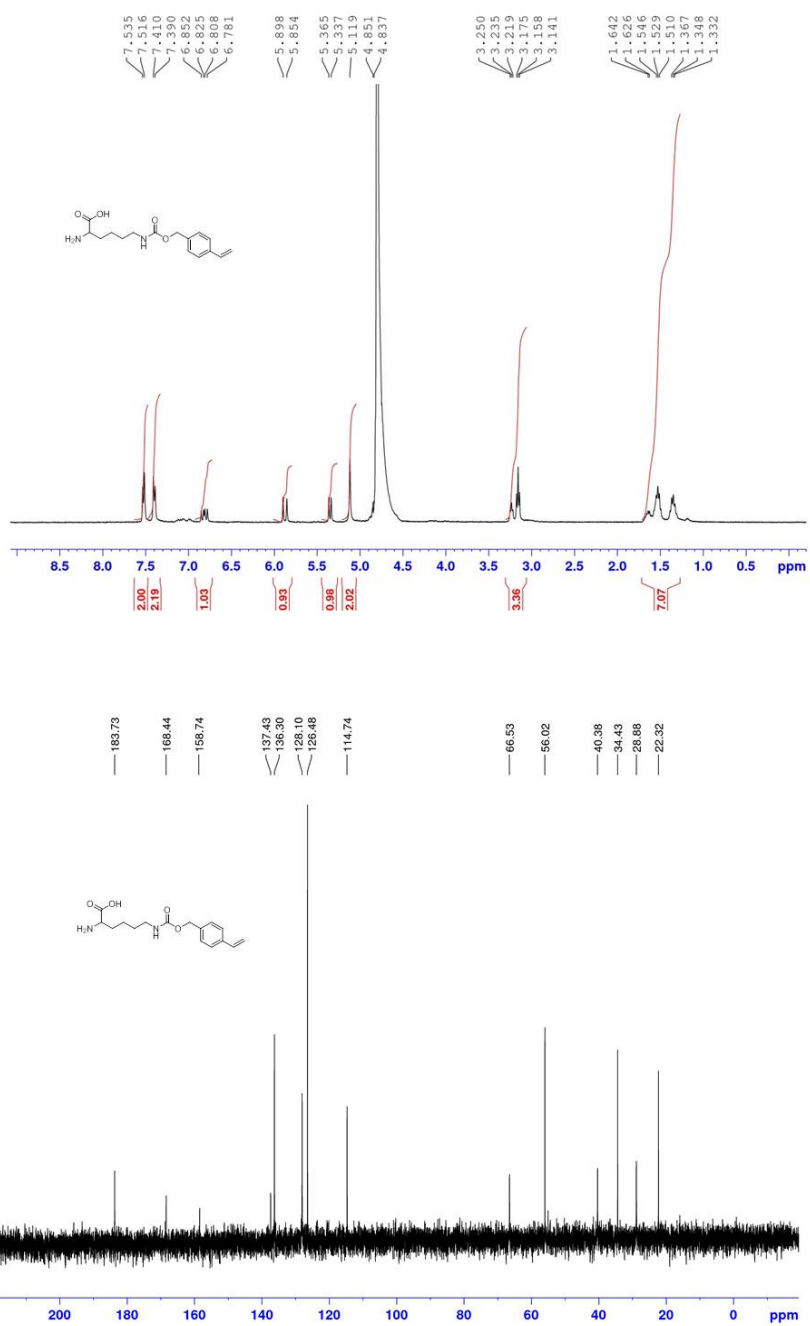


Figure S12. ¹H and ¹³C NMR spectra of KStyr.

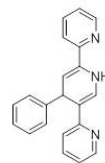
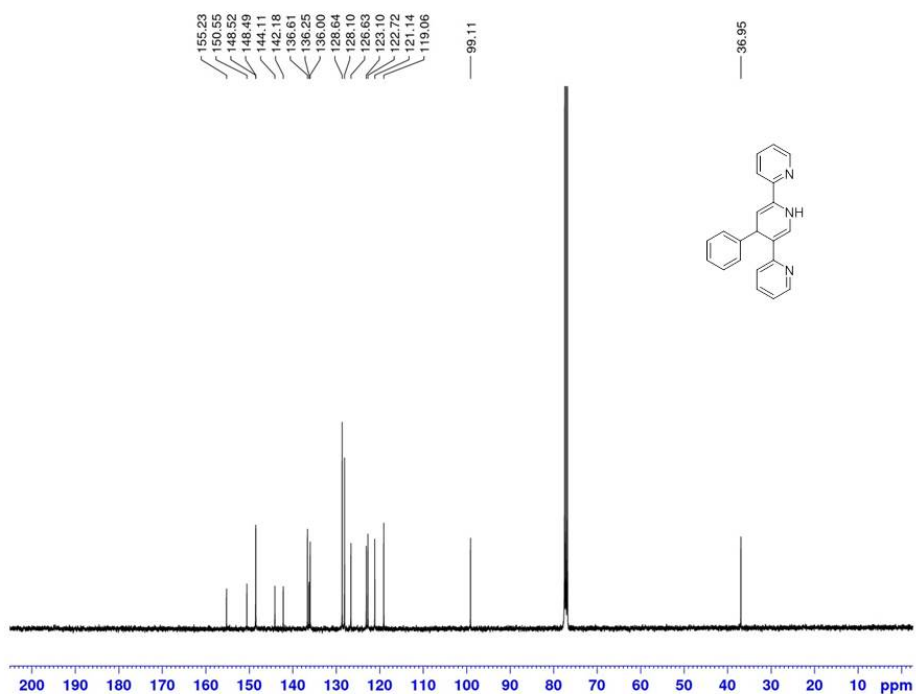
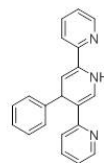
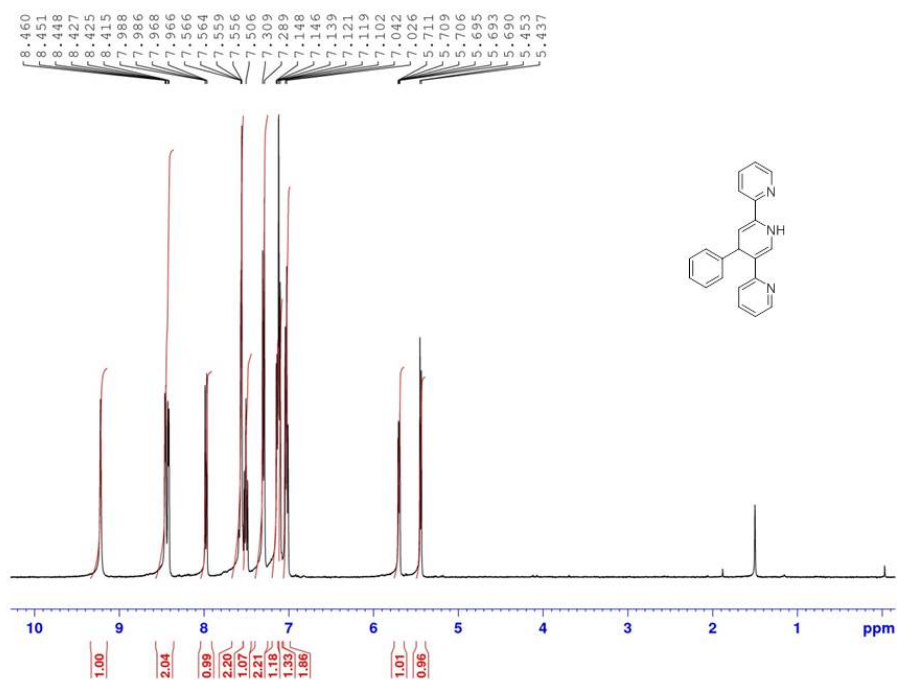


Figure S13. ¹H and ¹³C NMR spectra of 4-phenyl-3,6-di(pyridin-2-yl)-1,4-dihydropyridazine (PDHP).

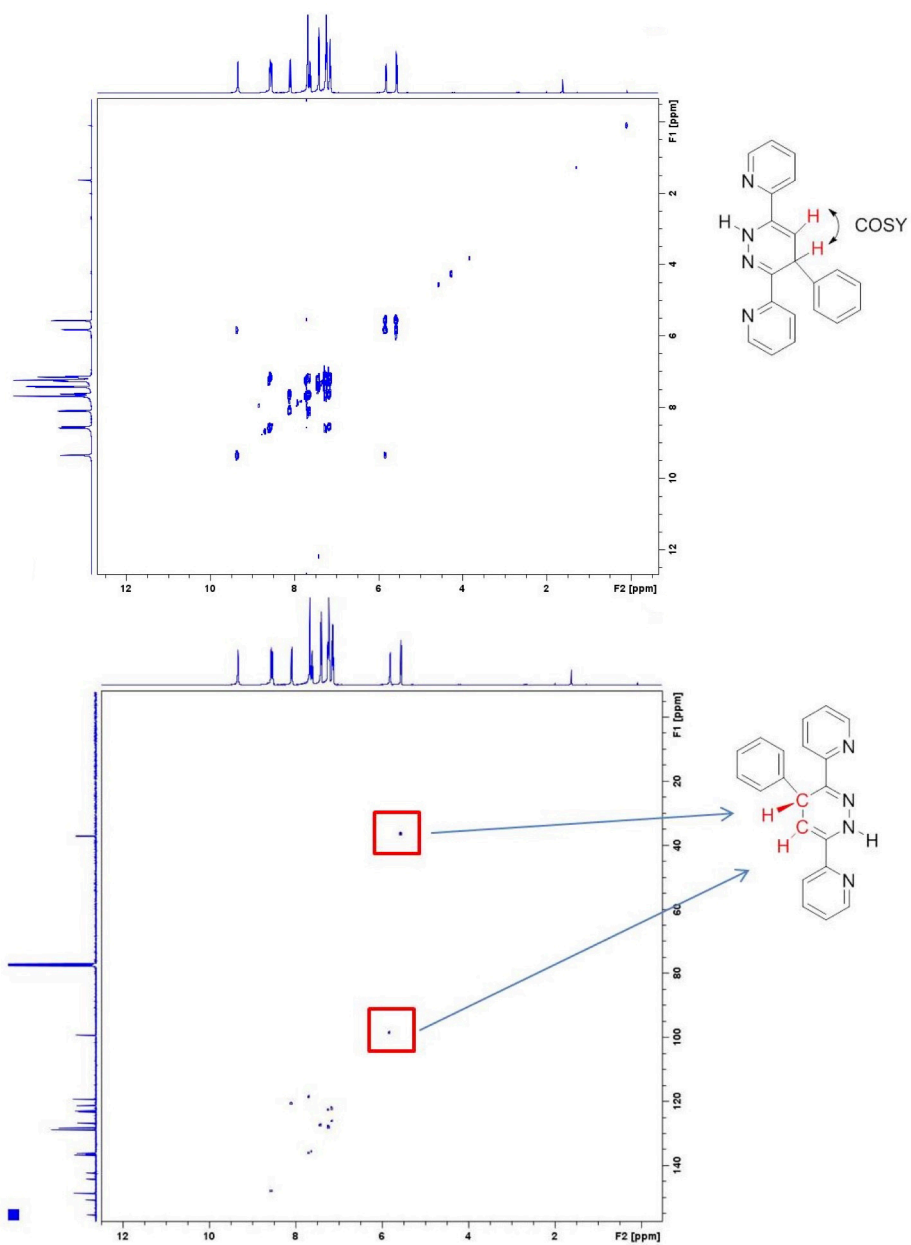


Figure S14. COSY and HSQC analyses of 4-phenyl-3,6-di(pyridin-2-yl)-1,4-dihydropyridazine (PDHP).

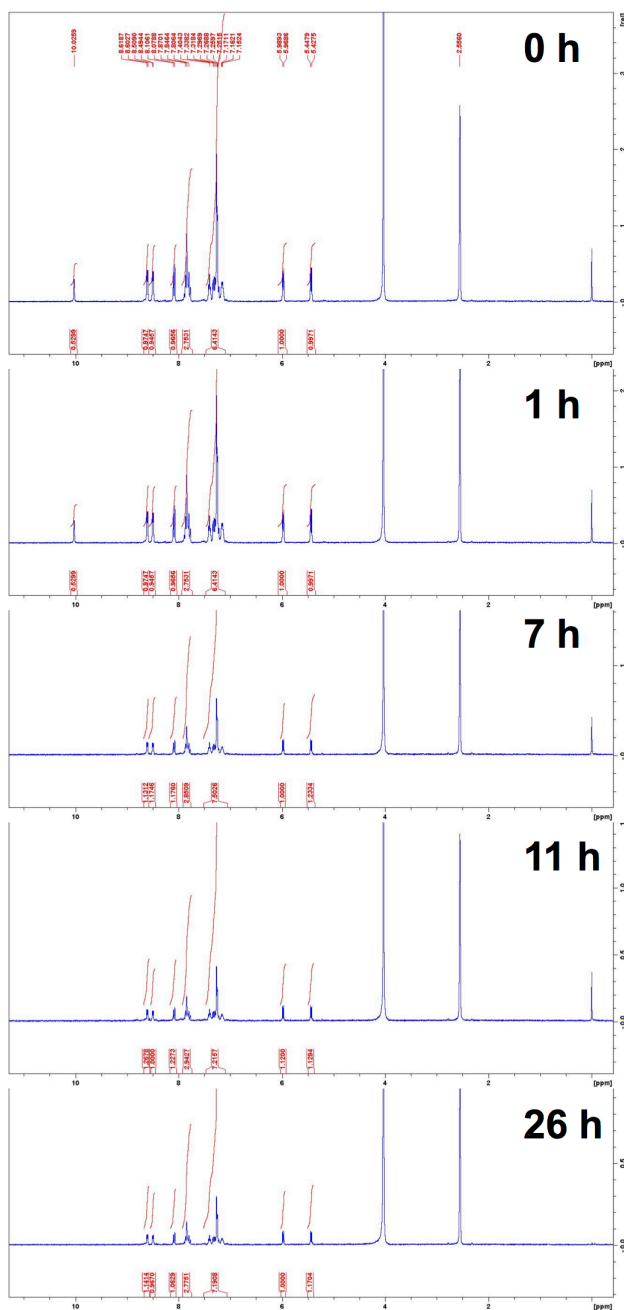


Figure S15. Stability study of PDHP in DMSO-d_6 . The solution was stored in NMR tube at room temperature ($21\text{ }^\circ\text{C}$) in $\text{DMSO/D}_2\text{O}$ (4:1). The ^1H NMR data was collected at indicated time points. PDHP stayed to be the major component after 26 hours. **Note:** We were unable to conduct the NMR stability study of PDHP in higher percentage of water due to the compound's limited solubility. In fact, PDHP crystals were formed during the incubation. More crystals were observed with longer incubation time. This was reflected in the decrease of the ^1H NMR signal. After 26 h, the crystals were collected and redissolved in $\text{DMSO/D}_2\text{O}$ (4:1) at $37\text{ }^\circ\text{C}$. Based on ^1H NMR, the crystals were still PDHP.

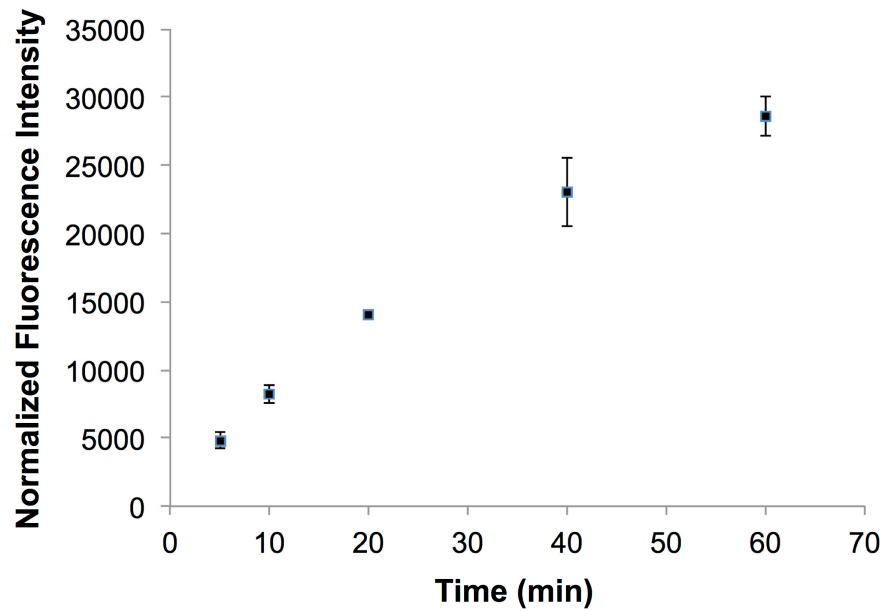


Figure 16. Reaction progress of sfGFP-N149KStyr labeling with 250 μ M of Tet. Following labeling reactions, protein samples were denatured by heating, analyzed by SDS-PAGE, and imaged by GE Typhoon imager (Excitation/Emission filter: LPB (510LP)). The fluorescence intensity of each labeled protein band was measured by ImageJ. The fluorescence intensity was normalized to the amount of protein.

References

1. Gierlich, J., Burley, G. A., Gramlich, P. M. E., Hammond, D. M., and Carell, T. *Org. Lett.* **2006**, *8*, 3639-3642.
2. Niu, Z., Bruckman, M., Kotakadi, V. S., He, J., Emrick, T., Russell, T. P., Yang, L., and Wang, Q. *Chem. Commun.* **2006**, 3019-3021.
3. Finney, N. S. *Curr. Opin. Chem. Biol.* **2006**, *10*, 238-245.
4. Li, Q., Lee, J.-S., Ha, C., Park, C. B., Yang, G., Gan, W. B., and Chang, Y.-T. *Angew. Chem., Int. Ed.* **2004**, *43*, 6331-6335.
5. Thellamurege, N. M., and Li, H. *J. Chem. Phys.* **2012**, *137*, 246101.
6. Thellamurege, N. M., Si, D., Cui, F., Zhu, H., Lai, R., and Li, H. *J. Comput. Chem.* **2013**, *34*, 2816-2833.
7. (a) Schmidt, M. W., Baldrige, K. K., Boatz, J. A., Elbert, S. T., Gordon, M. S., Jensen, J. H., Koseki, S., Matsunaga, N., Nguyen, K. A., and Su, S. *J. Comput. Chem.* **1993**, *14*, 1347-1363; (b) Gordon, M. S., and Schmidt, M. W. *Theory and Applications of Computational Chemistry: the first forty years* **2005**, 1167-1189.
8. Becke, A. D. *J. Chem. Phys.* **1993**, *98*, 5648-5652.
9. Wang, N., Ju, T., Niu, W., and Guo, J. *ACS Synth. Biol.* **2014**, *4*, 207-212.
10. Liu, X., Li, J., Hu, C., Zhou, Q., Zhang, W., Hu, M., Zhou, J., and Wang, J. *Angew. Chem., Int. Ed.* **2013**, *52*, 4805-4809.
11. Zhou, Z., and Fahrni, C. J. *J. Am. Chem. Soc.* **2004**, *126*, 8862-8863.
12. Lee, Y.-J., Kurra, Y., Yang, Y., Torres-Kolbus, J., Deiters, A., and Liu, W. R. *Chem. Commun.* **2014**, *50*, 13085-13088.
13. Rieder, U., and Luedtke, N. W. *Angew. Chem., Int. Ed.* **2014**, *53*, 9168-9172.
14. Wijnen, J. W., Zavarise, S., Engberts, J. B. F. N., and Charton, M. *J. Org. Chem.* **1996**, *61*, 2001-2005.
15. Lang, K., Davis, L., Torres-Kolbus, J., Chou, C., Deiters, A., and Chin, J. W. *Nat. Chem.* **2012**, *4*, 298-304.
16. Blackman, M. L., Royzen, M., and Fox, J. M. *J. Am. Chem. Soc.* **2008**, *130*, 13518-13519.
17. Patterson, D. M., Nazarova, L. A., Xie, B., Kamber, D. N., and Prescher, J. A. *J. Am. Chem. Soc.* **2012**, *134*, 18638-18643.
18. Kamber, D. N., Nazarova, L. A., Liang, Y., Lopez, S. A., Patterson, D. M., Shih, H. W., Houk, K. N., and Prescher, J. A. *J. Am. Chem. Soc.* **2013**, *135*, 13680-13683.
19. Baskin, J. M., Prescher, J. A., Laughlin, S. T., Agard, N. J., Chang, P. V., Miller, I. A., Lo, A., Codelli, J. A., and Bertozzi, C. R. *Proc. Natl. Acad. Sci. U. S. A.* **2007**, *104*, 16793-16797.
20. Lavis, L. D., and Raines, R. T. *ACS Chem. Biol.* **2008**, *3*, 142-155.